JOURNAL OF GUIDANCE, CONTROL, AND DYNAMICS
Vol. 19, No. 3, May–June 1996

Parametric Robustness Evaluation of a H_∞ Missile Autopilot

Gilles Ferreres*
Aérospatiale Missiles, 92320 Chatillon-sous-Bagneux, France
and
Mohammed M'Saad†
Laboratoire d'Automatique de Grenoble, 38402 St Martin d'Hères, France

A multivariable missile autopilot is synthesized using a H_∞ loop shaping procedure by McFarlane and Glover. Because missile flight control systems must guarantee stability and performance in the presence of large aerodynamic uncertainties, advanced μ tools are next used to analyze robust stability and performance of the control law in the presence of real parametric uncertainties in the stability derivatives. The multivariable H_∞ autopilot is proved to exhibit good parametric robustness properties. The control law is finally validated on a nonlinear simulator.

Nomenclature

d_2z, d_2y, ϕ	= normal and lateral accelerations and bank angle
d_2z_{co}, d_2y_{co}	= normal and lateral commanded accelerations
I_x, I_y, I_z	= roll, pitch, and yaw moments of inertia
m, V	= missile mass and inertial speed
p, q, r	= roll, pitch, and yaw rates
Z_x, Y_x, M_x, N_x, L_x	= stability derivatives; see Eq. (1)
α, β	= angle of attack and sideslip angle
η, ζ, ξ	= elevator, rudder, and aileron deflections

I. Introduction

THIS paper illustrates the application of recent robustness tools for the analysis and design of a missile autopilot. A multivariable H_∞ missile autopilot is first synthesized using McFarlane and Glover's procedure.[1–3] Advanced μ and ν tools[4–11] are next used to analyze robust stability and performance of the control law in the presence of real parametric uncertainties in the stability derivatives.[12,13] The missile autopilot is finally validated on a nonlinear simulator.

H_∞ techniques are classically used to achieve a tradeoff between performance and robustness objectives, by enforcing templates on closed-loop transfer functions.[13–16] An alternative to this method is a two-stage design procedure by McFarlane and Glover, in which the open loop plant is first shaped according to classical loopshaping rules.[1–3,17] A H_∞ robust stabilization procedure is then applied to the shaped plant, and a design indicator measures the degradation of the desired open-loop shape by the stabilizing controller.

As advantages of the stabilization procedure, unstable plant perturbations can be taken into account[18] and the controller is directly obtained without γ iterations. Moreover, the method generally avoids exact pole/zero cancellations[19] and balances to some extent the input/output performance and robustness properties.[3]

On the other hand, μ analysis provides a general framework for robustness analysis in the face of model uncertainties. An interval for the structured singular value (s.s.v.) μ is usually computed in practice using polynomial-time algorithms.[4–6]

New μ tools are nevertheless also available: μ sensitivities[7] can bring further information in addition to the basic application of μ analysis, whereas the ν tool[8–11] can directly solve skewed μ problems that would otherwise involve a recursive application of μ analysis (e.g., robust performance problems or direct computation of the maximal s.s.v. over the frequency range).

The use of these new μ tools consequently enables further investigation of the robustness properties of a controller beyond the basic application of the real/mixed μ tool. We first illustrate on the H_∞ missile autopilot that the ν measure can advantageously replace the s.s.v. in robust performance analysis. We then illustrate that the s.s.v., the ν measure, and the μ sensitivities can be combined so as to maximize in a rather systematical way the guaranteed domain of stability of the closed loop in the space of uncertainties.

The paper is organized as follows. Section II describes the design objectives and the missile model. Section III is a general presentation of the H_∞ design with coprime factors and loop shaping. Section IV briefly reviews the μ tools used in this paper, whereas Sec. V describes the design of the autopilot and a first analysis of the control law. Section VI is devoted to the parametric robustness analysis and to the validation of the autopilot on a nonlinear simulator. Concluding remarks end the paper.

II. Design Objectives and Missile Model

A skid-to-turn tail-controlled missile is considered. The goal of the autopilot is to control normal and lateral accelerations (pitch and yaw channels), while maintaining the bank angle to zero (roll channel). Rate outputs are also available for feedback. The primary design objective consists in ensuring the fastest tracking and regulation dynamics, while guaranteeing satisfactory robustness in the face of uncertain dynamics (actuators, bending modes, delays) and large aerodynamic uncertainties.

The simulation model essentially includes the nonlinear aerodynamic model, three nonlinear actuators, bending modes acting on the yaw and pitch channels, and Padé approximations, which model

Table 1 Dispersions for the three-axis autopilot

	$Z_\alpha - Y_\beta$, %	$M_\alpha - N_\beta$, %	$M_\eta - N_\xi$, %	L_α, %	L_β, %
Nominal disp.	±10	±20	±15	±40	±40
Margins (μ)	±27	±54	±41	±108	108
Margins (ν)	±27	±54	±41	±108	317
	L_ξ, %	$Z_q - Y_r$, %	$Z_\eta - Y_\zeta$, %	$M_q - N_r$, %	L_p, %
Nominal disp.	±20	±20	±15	±20	±20
Margins (μ)	±54	±54	±41	±54	±54
Margins (ν)	±54	±159	±41	±54	±159

Received Jan. 13, 1995; revision received Jan. 18, 1996; accepted for publication Jan. 26, 1996.

*Engineer, 2 à 18 rue Béranger; currently Research Scientist, Automatic Control Department, Centre d'Etudes et de Recherches de Toulouse, 2 Avenue Edouard Belin, BP 4025, 31055 Toulouse, France.
†Research Scientist, ENSIEG, BP 46.

the various delays in the loop. The actuators are more precisely modeled as second-order linear transfer functions with saturations on the outputs and on the first and second derivatives of the outputs with respect to time.

Considering one flight condition (Mach, altitude), a set of linear time-invariant models of the missile can be obtained by linearizing the aerodynamic model at various trim points corresponding to the range of variation of angles α and β.

The linearized dynamics of the missile can be described by the following simplified equations:

$$I_x \frac{dp}{dt} = L_\alpha \alpha + L_\beta \beta + L_p p + L_\xi \xi$$

$$I_y \frac{dq}{dt} = M_\alpha \alpha + M_q q + M_\eta \eta + (I_z - I_x) p_{eq} r + (I_z - I_x) r_{eq} p$$

$$I_z \frac{dr}{dt} = N_\beta \beta + N_r r + N_\zeta \zeta + (I_x - I_y) p_{eq} q + (I_x - I_y) q_{eq} p \quad (1)$$

$$\frac{d\alpha}{dt} = q - p_{eq}\beta - \beta_{eq} p + \frac{Z_\alpha \alpha + Z_q q + Z_\eta \eta}{mV}$$

$$\frac{d\beta}{dt} = -r + p_{eq}\alpha + \alpha_{eq} p + \frac{Y_\beta \beta + Y_r r + Y_\zeta \zeta}{mV}$$

where $(p_{eq}, q_{eq}, r_{eq}, \alpha_{eq}, \beta_{eq})$ denotes the values p, q, r, α, β at the trim point. One assumes that $I_y = I_z$ because of the symmetry of the missile.

The linearized models are thus characterized by the 16 stability derivatives describing the pitch channel (Z_α, Z_q, Z_η, M_α, M_q, M_η), the yaw channel (Y_β, Y_r, Y_ζ, N_β, N_r, N_ζ), and the roll channel (L_α, L_β, L_p, L_ξ). Dispersions on each of these 16 coefficients are prespecified (see Table 1).

III. Loop Shaping H_∞ Design

A. Robust Stabilization

The normalized left coprime factors $\tilde{M}(s)$ and $\tilde{N}(s)$ of a transfer matrix $G_0(s)$ are defined as

$$G_0(s) = \tilde{M}^{-1}(s)\tilde{N}(s) \quad (2)$$

where $\tilde{M}$ and $\tilde{N}$ are transfer matrices in RH_∞, which verify

$$\tilde{N}(s)\tilde{N}^T(-s) + \tilde{M}(s)\tilde{M}^T(-s) = I \quad (3)$$

Introducing additive perturbations on these coprime factors, a family of perturbed models can be defined as

$$\mathcal{G}_\epsilon = \left\{ G = (\tilde{M} + \Delta_M)^{-1}(\tilde{N} + \Delta_N), \right.$$
$$\left. \text{where} \quad \Delta_M, \Delta_N \in RH_\infty \quad \text{and} \quad \|[\Delta_M \ \ \Delta_N]\|_\infty < \epsilon \right\} \quad (4)$$

The family $\mathcal{G}_\epsilon$ defines a ball of center G_0 and radius ϵ in the topology induced by the gap metric.[20] Moreover, this family can contain unstable plants with a variable number of poles in the right half-plane.[18,20]

The aim of the robust stabilization procedure is to find the largest value of ϵ, denoted $\epsilon_{\max}$, such that a single fixed controller $K(s)$ stabilizes the whole family $\mathcal{G}_\epsilon$. As a striking advantage of McFarlane and Glover's procedure, it is possible to solve this particular H_∞ optimization problem directly, i.e., without γ iterations. The stability margin $\epsilon_{\max}$ is, indeed, explicitly known as

$$\epsilon_{\max}^2 = 1 - \|[\tilde{M} \ \ \tilde{N}]\|_H^2 \quad (5)$$

where $\| \ \|_H$ denotes the Hankel norm of a system. The practical computation of $\epsilon_{\max}$ and of a corresponding suboptimal controller essentially requires solving two Riccati equations.[1]

It is, however, not possible in this scheme to take into account performance objectives. This drawback can be bypassed by the preliminary use of loop shaping.

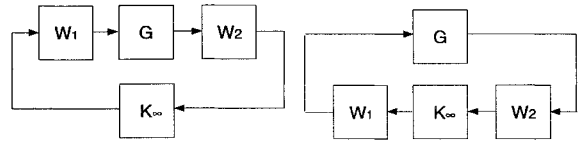

Fig. 1 H_∞ loop shaping.

B. Loop Shaping

We first briefly recall that it is possible to translate closed-loop objectives into open-loop ones, using the well-known approximate relations between closed-loop and open-loop transfer matrices.[17] For example, when supposing that $\bar{\sigma}(KG) \gg 1$ (typically at low frequencies), a performance objective on the sensitivity function can be translated into an open-loop objective on KG using the relation

$$\bar{\sigma}((I + KG)^{-1}) \simeq \frac{1}{\underline{\sigma}(KG)} \quad (6)$$

Classical tools such as integrators, proportional-integral (PI) controllers, or lead-lag or lag-lead filters are used in practice to shape the singular values of transfer matrices KG or GK.

Pre- and postcompensators W_1 and W_2 are consequently used to shape the open-loop plant $G(s)$ according to classical loop shaping rules. The shaped plant $G_S = W_2 G W_1$ is then stabilized using the procedure of the preceding section. The controller $K(s)$ is finally obtained as $W_1 K_\infty W_2$, where K_∞ is the controller provided by the stabilization procedure (see Fig. 1). Here, $\epsilon_{\max}$ provides a measure of the degradation of the loop shaping by the stabilizing controller.

Note, finally, that it is possible to reduce the controller $K(s)$, by directly reducing its coprime factors and to infer a guaranteed associated stability margin $\epsilon_r \leq \epsilon_{\max}$ (Ref. 1).

IV. μ and ν Tools for Robustness Analysis

A. Introduction

The aim of real/mixed μ analysis is to study robust stability or performance in the face of real parametric uncertainties and neglected dynamics. The closed-loop subject to model uncertainties is first transformed into the standard interconnection structure $M(s) - \Delta$ of Fig. 2, where all uncertainties are gathered in the structured model perturbation Δ. For the sake of simplicity, if one considers only parametric uncertainties, Δ becomes

$$\Delta = \text{diag}(\delta_i I_{qi}) \quad (7)$$

The real scalars δ_i represent the normalized parametric uncertainties, i.e., $\delta_i \in [-1, 1]$ represents the range of variations of the ith uncertain parameter within the prespecified dispersions. Introducing the unit hypercube D in the space of parametric uncertainties δ_i

$$D = \{\delta = [\delta_1 \cdots \delta_n] \mid \delta_i \in R \quad \text{and} \quad |\delta_i| \leq 1\} \quad (8)$$

μ analysis enables to compute the maximal amount of parametric uncertainties before destabilization of the closed loop, by computing the maximal value $k_{\max}$ of k, such that the interconnection structure of Fig. 2 is stable for all parametric uncertainties inside kD.

In practice, the s.s.v. $\mu[M(j\omega)]$ is usually computed as a function of frequency ω, and $k_{\max}$ is obtained as

$$k_{\max} = \min_\omega \frac{1}{\mu[M(j\omega)]} \quad (9)$$

Note that $1/\mu[M(j\omega)]$ can be interpreted as the size of the smallest parameter perturbation for which a closed-loop pole is obtained on the imaginary axis at $j\omega$, so that $k_{\max}$ represents the size of the smallest perturbation for which a closed-loop pole is obtained on the imaginary axis.

For notational convenience, we leave out the ω dependence in the following, so that M denotes the complex matrix $M(j\omega)$ at frequency ω.

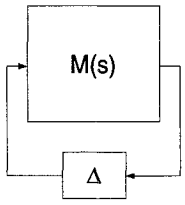

Fig. 2 Interconnection structure.

B. Definition of μ and ν

Consider now the general case of mixed uncertainties and split the structured perturbation Δ into two structured perturbations Δ_1 and Δ_2. Consequently, Δ_i is a block diagonal matrix, which contains real scalars δ_i (representing the parametric uncertainties) and full complex blocks, which represent either neglected dynamics or performance blocks. Introducing the unit ball $B\Delta$ as

$$B\Delta = \{\Delta = \text{diag}(\Delta_1, \Delta_2) \mid \bar{\sigma}(\Delta) \leq 1\} \tag{10}$$

The s.s.v., $\mu(M)$, associated with this problem is classically defined as

$$\begin{aligned} \mu(M) &= 1/\min[k/\exists \Delta \in kB\Delta \quad \text{with} \quad \det(I - M\Delta) = 0] \\ &= 0 \qquad \text{if no} \qquad (k, \Delta) \qquad \text{exists} \end{aligned} \tag{11}$$

The related quantity, $\nu(M)$, can now be defined as

$$\begin{aligned} \nu(M) &= 1/\min[k/\exists \Delta = \text{diag}(\Delta_1, k\Delta_2) \\ &\text{with} \quad \Delta_i \in B\Delta_i \quad \text{and} \quad \det(I - M\Delta) = 0] \end{aligned} \tag{12}$$

When computing μ, the unit ball $B\Delta$ is expanded (or shrunk) by factor k until the matrix $I - M\Delta$ becomes singular for a structured perturbation Δ inside $kB\Delta$. When computing the skewed s.s.v. ν, the unit ball $B\Delta_2$ (in the space of structured perturbations Δ_2) is expanded (or shrunk) by factor k, but the structured perturbation Δ_1 remains now inside the unit ball $B\Delta_1$.

The usefulness of the ν measure will be illustrated in Sec. VI; see also Refs. 9–11.

C. μ Sensitivities

Without loss of generality, we assume to analyze the sensitivity of the s.s.v. $\mu(M)$ with respect to the first block. We introduce the scalar α and define

$$M(\alpha) = \begin{bmatrix} \alpha M_{11} & \sqrt{\alpha} M_{12} \\ \sqrt{\alpha} M_{21} & M_{22} \end{bmatrix} \tag{13}$$

where M is partitioned so that M_{11} corresponds to the first block and M_{22} to the other blocks of Δ.

The μ sensitivity with respect to the first block is defined as

$$\delta\mu = \lim_{\Delta\alpha \to 0^+} \left. \frac{\mu[M(\alpha)] - \mu[M(\alpha - \Delta\alpha)]}{\Delta\alpha} \right|_{\alpha = 1} \tag{14}$$

It is easily proven that $\mu[M(\alpha)]$ is a nondecreasing function of α, so that $\delta\mu$ is necessarily nonnegative. Moreover, it can be proven that the μ sensitivities are well defined and equal to the corresponding full derivatives almost everywhere on any interval of variation of α (Ref. 7).

D. Mixed ν Upper Bound

A mixed ν upper bound is extracted from Refs. 9 and 10. With the notations of Refs. 5 and 10, we first introduce the hermitian structured matrix G associated with perturbation $\Delta = \text{diag}(\Delta_1, \Delta_2)$ and the scaling matrices $\underline{D}_i$ associated with perturbations Δ_i. D_1 and D_2 are then defined as

$$D_1 = \begin{bmatrix} \underline{D}_1 & 0 \\ 0 & 0 \end{bmatrix} \qquad D_2 = \begin{bmatrix} 0 & 0 \\ 0 & \underline{D}_2 \end{bmatrix} \tag{15}$$

so that $D = D_1 + D_2$ is a scaling matrix associated with perturbation Δ. Considering then two hermitian matrices A and B, with $B \geq 0$, $\eta(A, B)$ is finally defined as

$$\eta(A, B) = \sup[\gamma \in R : \bar{\lambda}(A - \gamma B) \geq 0] \tag{16}$$

Result: A ν upper bound is given by

$$\nu(M) \leq \nu_{UB}(M) = \min_{D_1, D_2, G} \sqrt{\max[0, \eta(H, D_2)]} \tag{17}$$

where $H = M^*(D_1 + D_2)M - D_1 + j(GM - M^*G)$.

Remark: $\eta(A, B)$ is almost always equal to the generalized eigenvalue $\bar{\lambda}(A, B)$, except possibly when $\eta(A, B) = +\infty$ (see Proposition 5.1.c. of Ref. 8). In the same way as the mixed μ upper bound of Ref. 5, this mixed ν upper bound can thus be computed in practice using recent methods for solving linear matrix inequalities.[21]

V. Design of the Autopilot

A. Control Objectives

The linearized closed loop must verify the following specifications:

1) Minimal values for rising time, overshoot, and decoupling are required for the step response.

2) The autopilot must avoid saturating the actuators as much as possible (saturations on the actuators outputs and their first and second derivatives).

3) The autopilot must tolerate additive perturbations of +40 dB at $\omega > 0.8\omega_{bm}$, where ω_{bm} is the eigenfrequency of the bending mode. This template corresponds to uncertainties of $\pm 30\%$ on the eigenfrequency and $\pm 70\%$ on the damping ratio of the bending mode.

4) The multivariable input margins must be satisfactory. The first two specifications must also be verified in final simulation with the complete nonlinear model.

B. Choice of the Pre- and Postcompensators

The pre- and postcompensators W_1 and W_2 are chosen as follows:

$$\begin{aligned} W_1 &= 1/(1 + \tau s)\, \text{diag}(W_{11}, W_{11}, k_r) \\ W_2 &= \text{diag}(W_{2PY}, W_{2PY}, W_{2R}) \end{aligned} \tag{18}$$

where

$$W_{11} = k_{PY} \frac{s^2/\omega_1^2 + 2\xi_1/\omega_1 s + 1}{s^2/\omega_1^2 + 1.4/\omega_1 s + 1} \tag{19}$$

$$\begin{aligned} W_{2PY} &= \begin{bmatrix} s^{-1} & 0 \\ 0 & k_q \dfrac{1 + \tau_1 s}{1 + \tau_2 s} \end{bmatrix} \\ W_{2R} &= \begin{bmatrix} k_\phi[1 + (\omega_I/s)] & 0 \\ 0 & k_p \end{bmatrix} \end{aligned} \tag{20}$$

The first-order transfer function $1/(1 + \tau s)$ is used to increase the rolloff, so as to ensure good immunity in the presence of high-frequency noise. In addition to the rolloff, notch filters $W_{11}(\omega_1 = 0.85\omega_{bm}$ and $\xi_1 = 0.05)$ are added in the precompensator for robustness in the face of uncertain bending modes. For low-frequency performance, the postcompensator includes simple integrators on the acceleration outputs and a proportional-integral controller on the bank angle output. Lag-lead filters are finally added on the pitch and yaw rate outputs, so as to ensure a -20 dB/decade rate of the singular values at middle frequencies.

The loop shaping is followed by an application of the stabilization procedure. The obtained value of ϵ_{max} is 0.29. Figures 3 and 4 show the singular values of the shaped plant (before stabilization) and the open-loop singular values obtained at the inputs after stabilization. The loop shaping is rather slightly degradated. The order of the controller is 36 (6 for the aerodynamic model, plus 6 for the actuators, plus 2×12 for the weightings W_1 and W_2). After a balanced model reduction, the order of the final controller is reduced to 22, and the new stability margin is $\epsilon_r = 0.27$.

C. Analysis

Multivariable input margins are first computed as 30.7 deg and 6.1 dB. The robustness of the autopilot in the presence of uncertain bending modes is then analyzed. Figure 5 shows the complex s.s.v. corresponding to four additive model perturbations on the outputs of the pitch and yaw channels. It can be checked on this figure that the corresponding design objective of Sec. V.A is achieved. These results confirm the good quality of the loop shape of Sec. V.B.

Robust stability and performance in the face of large aerodynamic uncertainties are analyzed in the following section. Note that the condition provided by μ analysis can be considered as a necessary condition, when applied to the nonlinear plant.

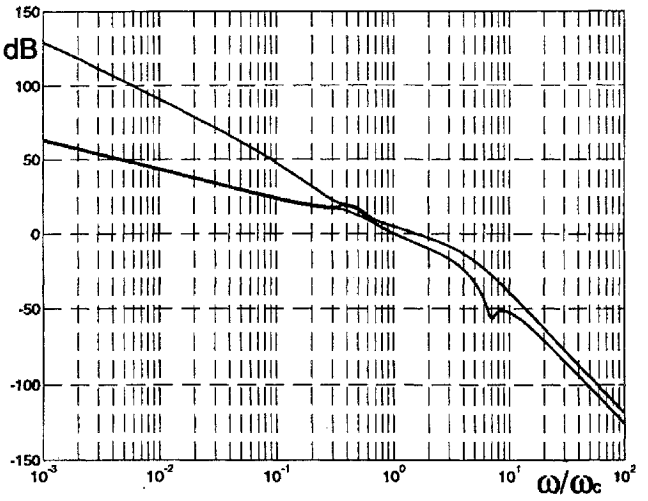

Fig. 3 Singular values of the shaped plant.

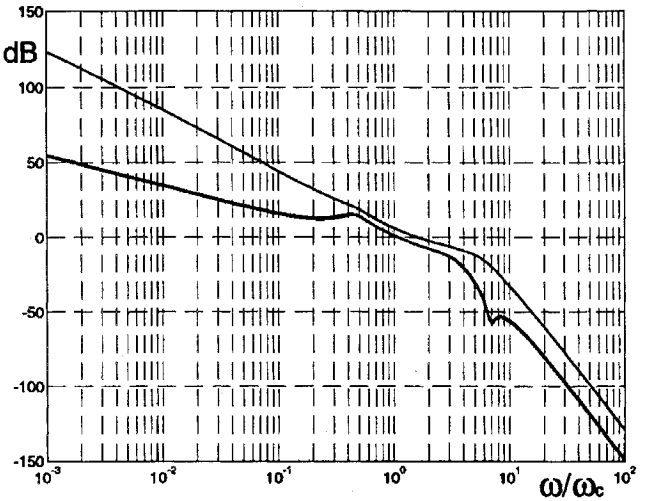

Fig. 4 Open-loop singular values (KG).

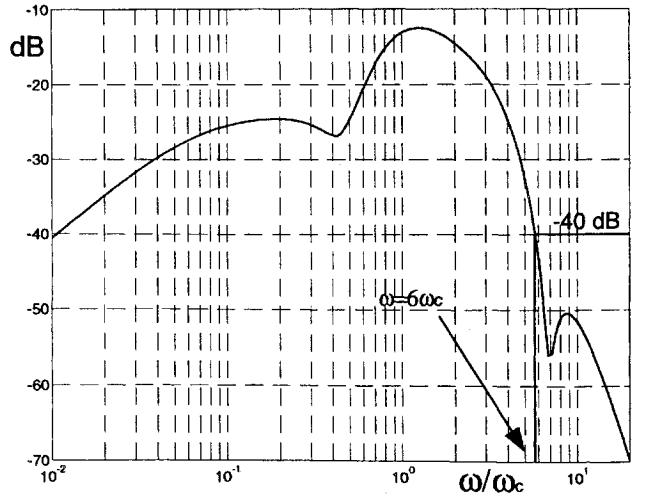

Fig. 5 Robustness in the face of bending modes.

VI. Robustness Analysis

The μ and ν tools are now applied to the robustness analysis of the missile autopilot. We first illustrate that the ν measure can advantageously replace the s.s.v. for robust performance analysis. A combination of the s.s.v., the ν measure, and the μ sensitivities is next used to maximize the guaranteed domain of stability in the space of uncertain parameters.

As a preliminary, the prespecified dispersions on each of the 16 stability derivatives (see Table 1) are used to normalize the variations of these parameters. The standard interconnection structure of Fig. 2 is then built with Morton's method[22] (see also Ref. 13.) The feedback uncertainty block Δ only contains nonrepeated real uncertainties (and full complex blocks for the robust performance problem).

A. Robust Performance

Consider a plant subject to a structured model perturbation Δ_P. We would like to verify whether the sensitivity function S verifies a template $1/W_1$ despite the model uncertainties. Let $\tilde{S}$ be the sensitivity function of the closed-loop subject to perturbation Δ_P. We are more precisely interested in computing the largest value $k_{\max}$ of k, such that $\|W_1\tilde{S}\|_\infty \leq 1$ for all uncertainties Δ_P of size less than or equal to k.

A fictitious complex block Δ_C is classically added and an augmented perturbation $\Delta = \text{diag}(\Delta_P, \Delta_C)$ is considered. The computation of $k_{\max}$ is a ν problem, since the goal is to maintain Δ_C inside its unit ball and to expand or shrink the unit ball $B\Delta_P$ by the maximal allowable value of k.

A second problem of interest can also be considered: One now maintains Δ_P inside its unit ball, while maximizing the size of Δ_C. The maximal value of α is then obtained, such that $\|W_1\tilde{S}\|_\infty \leq 1/\alpha$ for all uncertainties Δ_P of size less or equal to 1.

Summarizing the approach, the performance requirement is maintained constant in the first problem and the size of the uncertainties are maximized, for which robust performance is guaranteed. In the second problem, the performance requirement is maximized for a given amount of uncertainties.

We now analyze robustness of the shaping on the sensitivity function S in the face of uncertainties in the 16 stability derivatives. We are more precisely interested in the transfer matrix between (d_2z_{co}, d_2y_{co}) and $(d_2z_{co} - d_2z, d_2y_{co} - d_2y)$. The template on S is defined as $\text{diag}(W_{SP}, W_{SY})$, where W_{SP} and W_{SY} are second-order transfer functions, characterized by a minimal required bandwidth and a maximal overshoot for S.

Figure 6 shows the corresponding mixed s.s.v. Note on the figure that, as expected, the two upper bounds of Refs. 5 and 6 nearly coincide at all frequencies (see Ref. 13 for further details). A tight interval for the maximal s.s.v. is obtained as [0.92, 0.93] at $\omega = 0.23\omega_c$, so

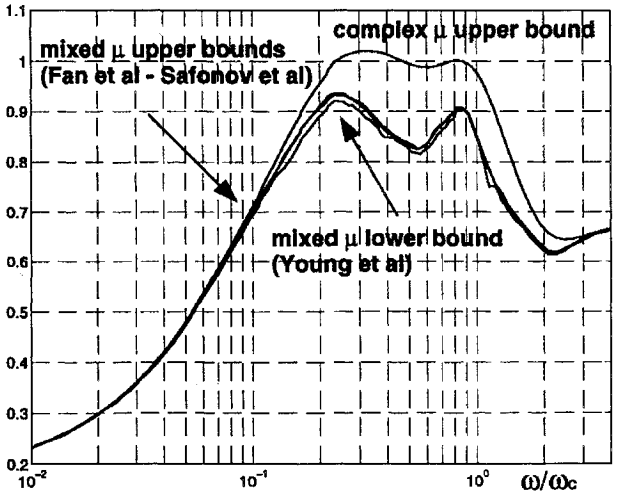

Fig. 6 Robust performance; μ analysis.

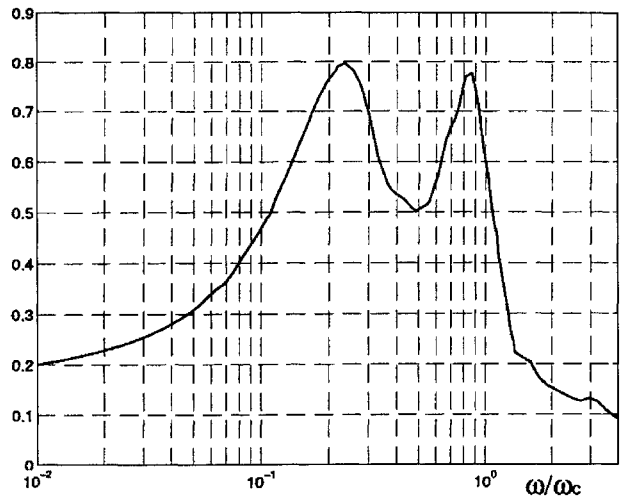

Fig. 7 Robust performance; ν analysis.

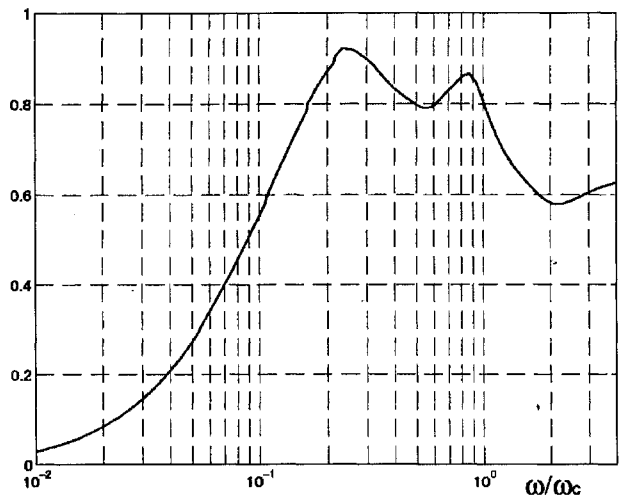

Fig. 8 Robust performance; ν analysis.

that robust performance is guaranteed for the prespecified dispersions of parameters.

Figure 7 shows the ν upper bound corresponding to the first problem described at the beginning of the section. The maximal value of the ν upper bound is obtained as 0.79 at $\omega = 0.23\omega_c$, so that robust performance is guaranteed for the prespecified parameter dispersions, multiplied by a factor $k_{\max} = 1/0.79 = 1.27$. Figure 8 shows the ν upper bound corresponding to the dual problem. The maximal value is obtained as 0.92 at $\omega = 0.23\omega_c$, so that the template on S can be divided by 0.92 while still guaranteeing robust performance for the prespecified dispersions.

B. Robust Stability

We first illustrate the approach on a simplified example, by considering the case where Δ_1 and Δ_2 correspond to two real parametric uncertainties in the stability derivatives N_r and N_ζ. Figure 9 shows the domain of stability of the closed loop in the space of Δ_1 and Δ_2 (the variations Δ_1 and Δ_2 of N_r and N_ζ are normalized, so that $\Delta_1 = 1$ and $\Delta_2 = 1$ corresponds to a dispersion of +20% for N_r and +15% for N_ζ; see Table 1).

The μ analysis provides the largest square in the parameter space, such that stability of the closed loop is guaranteed inside this square. The ν tool, however, provides the largest rectangle in the parameter space, such that stability is guaranteed inside this rectangle.

The s.s.v. and the ν measure may, however, provide the same domain of stability, e.g., in the case of Fig. 10. In practice, μ analysis is first applied. The μ sensitivities are then computed to detect whether we are in the situation of Fig. 9 or Fig. 10. In the situation of Fig. 9, the guaranteed domain of stability of the closed loop in the space of uncertain parameters is further extended using the ν tool.

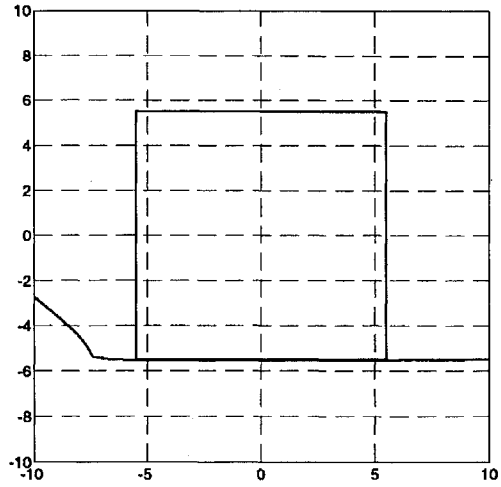

Fig. 9 Stability domain in the space of (N_r, N_ζ).

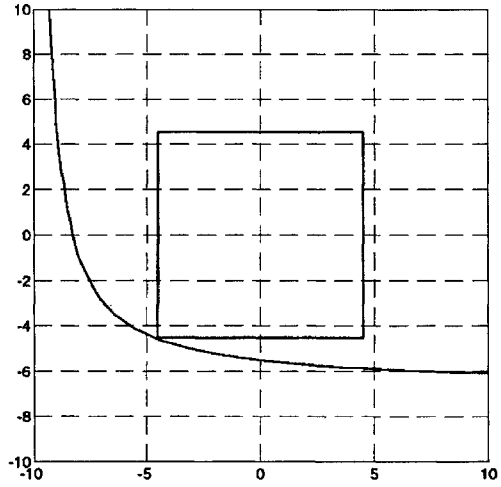

Fig. 10 Stability domain in the space of (Y_β, N_ζ).

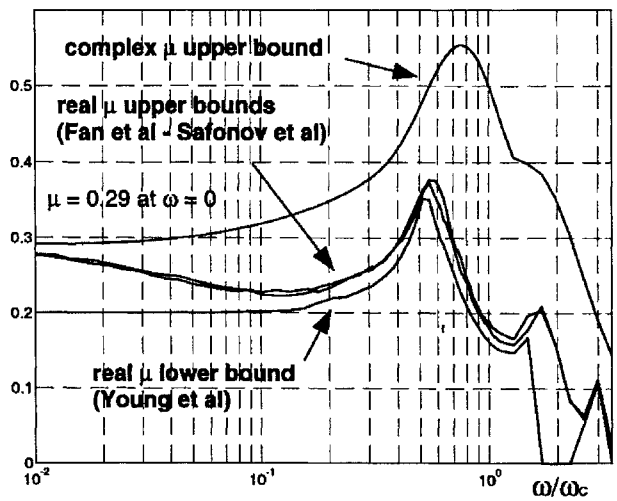

Fig. 11 Robust stability; μ analysis.

We now analyse robust stability in the face of uncertainties in the 16 stability derivatives. The maximal s.s.v. over the frequency range is obtained as $\mu_{\max} = 0.37$ (more exactly between 0.35 and 0.37) at $\omega = 0.55\omega_c$ (see Fig. 11). Table 1 lists the corresponding dispersions in the stability derivatives.

The μ sensitivities are then computed for each parameter. Figure 12 shows the example of the μ sensitivity corresponding to the stability derivative L_ξ. The μ sensitivities corresponding to the stability derivatives Z_q, Y_r, L_β, and L_p are shown to be large when compared to the μ sensitivities corresponding to the other stability derivatives.

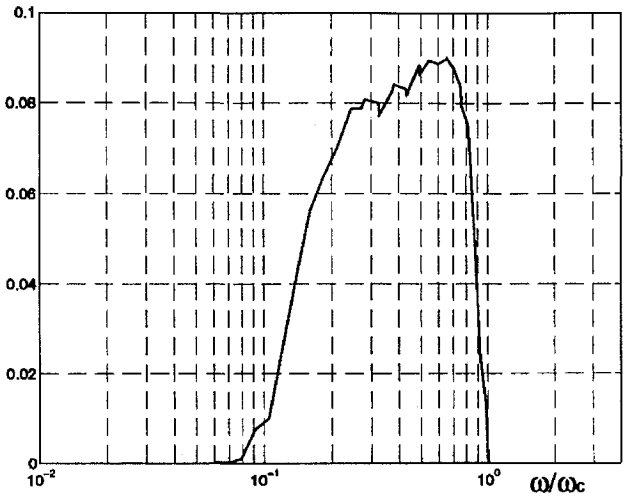

Fig. 12 Example of μ sensitivity for L_ξ.

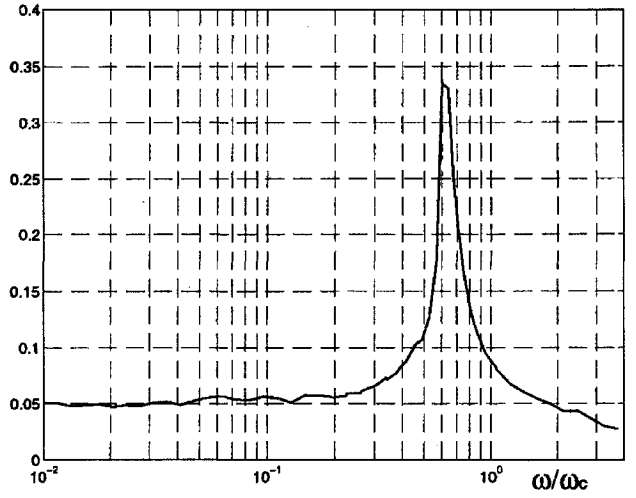

Fig. 13 Robust stability; ν analysis.

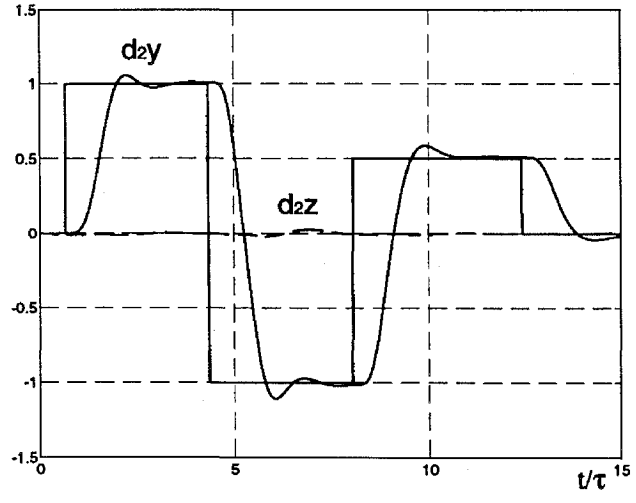

Fig. 14 Acceleration outputs.

After multiplication of the prespecified dispersions by a factor $0.99/\mu_{\max}$, we include in Δ_2 uncertainties in the stability derivatives Z_q, Y_r, L_β, and L_p, while the uncertainties in the other stability derivatives are included in Δ_1. Figure 13 shows the corresponding ν upper bound. The maximal value is obtained as $\nu_{\max} = 0.34$ at $\omega = 0.60\omega_c$. Table 1 lists the new maximal allowable dispersions.

C. Nonlinear evaluation

The complete nonlinear simulator is finally used to validate the design. Figures 14–17 show the missile response to a sequence of commanded lateral acceleration step changes. Specifications in terms of rising time, overshoot, and decoupling are verified, while the actuator outputs and their first and second derivatives with respect to time remain below the saturation values.

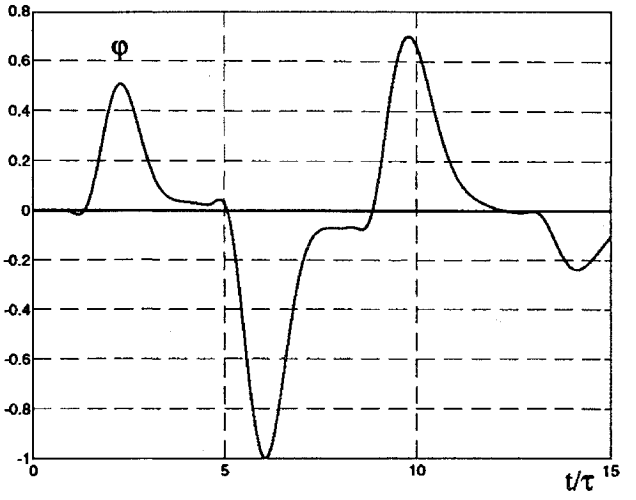

Fig. 15 Bank angle output.

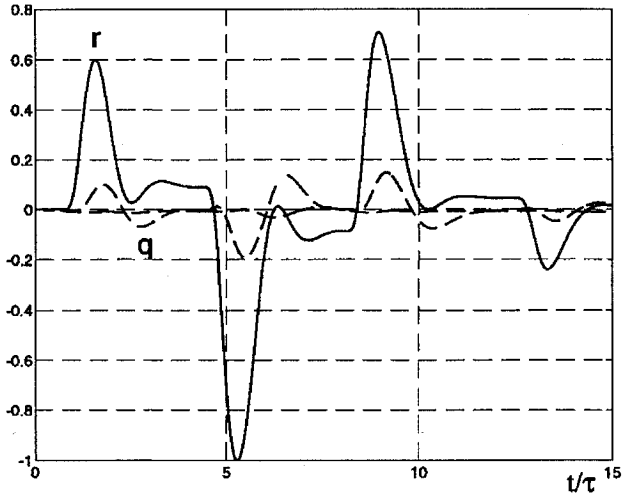

Fig. 16 Rate outputs.

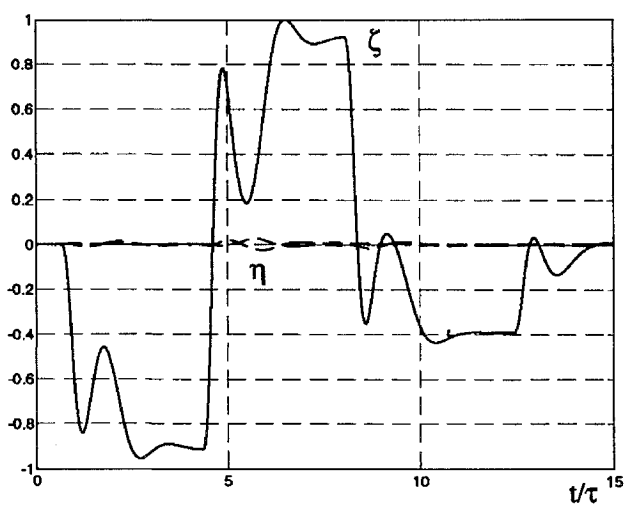

Fig. 17 Controller outputs.

Acknowledgment

The first author is grateful to Vincent Fromion (Ecole Supérieure d'Electricité—France) for fruitful discussions and valuable comments.

References

[1]McFarlane, D., and Glover, K., *Robust Controller Design Using Normalized Coprime Factor Plant Descriptions*, Lecture Notes in Control and Information Sciences, Springer–Verlag, Berlin, 1990.

[2]McFarlane, D. C., and Glover, K., "A Loop Shaping Design Procedure Using H_∞ Synthesis," *IEEE Transactions on Automatic Control*, Vol. 37, No. 6, 1992, pp. 759–769.

[3]Glover, K., Sefton, J., and McFarlane, D. C., "A Tutorial on Loop Shaping Using H-Infinity Robust Stabilization," *Proceedings of the IFAC World Congress*, 1990, pp. 94–103.

[4]Young, P. M., and Doyle, J. C., "Computation of μ with Real and Complex Uncertainties, *Proceedings of the IEEE Conference on Decision and Control*, 1990, pp. 1230–1235.

[5]Fan, M. K. H., Tits, A. L., and Doyle, J. C., "Robustness in the Presence of Mixed Parametric Uncertainty and Unmodeled Dynamics," *IEEE Transactions on Automatic Control*, Vol. 36, No. 1, 1991, pp. 25–38.

[6]Safonov, M. G., and Lee, P. H., "A Multiplier Method for Computing Real Multivariable Stability Margins," *Proceedings of the IFAC World Congress*, 1993, pp. 275–278.

[7]Braatz, R. P., and Morari, M., "μ Sensitivities as an Aid for Robust Identification," *Proceedings of the American Control Conference*, 1991, pp. 231–236.

[8]Fan, M. K. H., and Tits, A. L., "A Measure of Worst-Case H_∞ Performance and of Largest Acceptable Uncertainty," *Systems and Control Letters*, Vol. 18, No. 6, 1992, pp. 409–421.

[9]Ferreres, G., and M'Saad, M., "Direct Computation of the Maximal s.s.v. over the Frequency Range Using the ν Tool," *Proceedings of the IEEE Conference on Decision and Control*, 1994.

[10]Ferreres, G., and Fromion, V., "Computation of the Robustness Margin with the Skewed μ Tool," *Systems and Control Letters* (submitted for publication).

[11]Ferreres, G., and Fromion, V., "Skewed μ Problems in Robustness Analysis," *Automatica* (submitted for publication).

[12]Wise, K. A., "A Comparison of Six Robustness Tests Evaluating Missile Autopilot Robustness to Uncertain Aerodynamics," *Proceedings of the American Control Conference*, 1990, pp. 755–763.

[13]Ferreres, G., Fromion, V., Duc, G., and M'Saad, M., "Application of Real/Mixed μ Computational Techniques to a H_∞ Missile Autopilot," *International Journal of Robust and Nonlinear Control* (to be published).

[14]Reichert, R. T., "Robust Autopilot Design for Aircraft with Multiple Lateral-Axes Controls Using H_∞ Synthesis," *Proceedings of the IEEE Conference on Decision and Control*, 1990, pp. 2987–2992.

[15]Jackson, P., "Applying μ Synthesis to Missile Autopilot Design," *Proceedings of the IEEE Conference on Decision and Control*, 1990, pp. 2993–2998.

[16]Wise, K. A., Mears, B. C., and Poola, K., "Missile Autopilot Design Using H_∞ Optimal Control with μ Synthesis," *Proceedings of the American Control Conference*, 1990, pp. 2362–2367.

[17]Doyle, J. C., and Stein, G., "Multivariable Feedback Design: Concepts for a Classical/Modern Synthesis," *IEEE Transactions on Automatic Control*, Vol. 26, No. 1, 1981, pp. 4–16.

[18]Kwakernaak, H., "Robust Control and H_∞ Optimization—Tutorial Paper," *Automatica*, Vol. 29, No. 2, 1993, pp. 255–273.

[19]Tsai, M. C., Geddes, E. J. M., and Postlethwaite, I., "Pole-Zero Cancellations and Closed-Loop Properties of an H_∞ Mixed Sensitivity Design Problem," *Automatica*, Vol. 28, No. 3, 1992, pp. 519–530.

[20]Georgiou, T. T., and Smith, M. C., "Optimal Robustness in the Gap Metric," *IEEE Transactions on Automatic Control*, Vol. 35, No. 6, 1990, pp. 673–686.

[21]Boyd, S., El Ghaoui, L., Feron, E., and Balakrishnan V., *Linear Matrix Inequalities in Systems and Control Theory*, Society for Industrial and Applied Mathematics, 1994.

[22]Morton, B. G., "New Applications of μ to Real Parameter Variation Problems," *Proceedings of the IEEE Conference on Decision and Control*, 1985, pp. 233–238.